Allosteric communication between ligand binding domains modulates substrate inhibition in adenylate kinase

David Scheerer[a!], Bharat V. Adkar[b!], Sanchari Bhattacharyya[b], Dorit Levy[a], Marija Iljina[a], Inbal Riven[a], Orly Dym[a], Gilad Haran[a*] and Eugene I. Shakhnovich[b*]

[a] Department of Chemical and Biological Physics, Weizmann Institute of Science, Rehovot 761001, Israel
[b] Department of Chemistry and Chemical Biology, Harvard University, 12 Oxford St, Cambridge, MA 02138
! equal contribution

***Corresponding authors**: Gilad Haran (email: gilad.haran@weizmann.ac.il) and Eugene I. Shakhnovich (email: shakhnovich@chemistry.harvard.edu).

Author Contributions: Author Contributions: D.S., B.V.A., S.B., E.S. and G.H. designed research; D.S., B.V.A., S.B., M. I. and O.D. performed research; B.V.A., D.L. and I.R. expressed and purified the proteins; D.S., B.V.A., E.S. and G.H. analyzed data; and D.S., B.V.A., S.B., E.S. and G.H. wrote the paper.
Competing Interest Statement: The authors declare no competing interest.
Classification: Biological Sciences, Biophysics and Computational Biology.
Keywords: smFRET, enzymatic activity, protein dynamics.

This PDF file includes:

Main Text
Figures 1 to 4

Abstract

Enzymes play a vital role in life processes; they control chemical reactions and allow functional cycles to be synchronized. Many enzymes harness large-scale motions of their domains to achieve tremendous catalytic prowess and high selectivity for specific substrates. One outstanding example is provided by the three-domain enzyme adenylate kinase (AK), which catalyzes phosphotransfer between ATP to AMP. Here we study the phenomenon of substrate inhibition by AMP and its correlation with domain motions. Using single-molecule FRET spectroscopy, we show that AMP does not block access to the ATP binding site, neither by competitive binding to the ATP cognate site nor by directly closing the LID domain. Instead, inhibitory concentrations of AMP lead to a faster and more cooperative domain closure by ATP, leading in turn to an increased population of the closed state. The effect of AMP binding can be modulated through mutations throughout the structure of the enzyme, as shown by the screening of an extensive AK mutant library. Mutation of multiple conserved residues leads to increased substrate inhibition, suggesting a positive selection during evolution. Combining these insights, we developed a model that explains the complex activity of AK, particularly substrate inhibition, based on the experimentally observed opening and closing rates. Notably, the model indicates that the catalytic power is affected by the microsecond balance between the open and closed states of the enzyme. Our findings highlight the crucial role of protein motions in enzymatic activity.

Significance Statement

How conformational dynamics affect the catalytic activity of enzymes remains a topic of active debate. We focus here on the domain closure dynamics of adenylate kinase (AK) and how they are affected by substrate inhibition. By screening an extensive mutant library, we show that this feature of the enzyme has been under positive evolutionary selection. Importantly, domain closure is required in order to bring AK's substrates close together for their chemical reaction; single-molecule FRET studies directly measure the populations of the open and closed states. We find that overpopulation of the closed state can be detrimental to activity. The results allow us to develop a kinetic model that properly accounts for AK kinetics by combining conformational dynamics and biochemical steps.

INTRODUCTION

Enzymes have been designed by nature to accelerate vital chemical reactions by many orders of magnitude. Quite a few of them have evolved to harness large-scale motions of domains and subunits to promote their activity. The study of the structural dynamics of these proteins is essential to decipher how they function and are regulated, as has been demonstrated in multiple experimental and theoretical reports (1-4). The enzyme adenylate kinase (AK) is a paradigmatic example of a strong relation between conformational dynamics and catalytic activity (5-8). AK plays a key role in maintaining ATP levels in cells by catalyzing the reaction ATP + AMP ⇄ ADP + ADP. It consists of three domains: the large CORE domain, the LID domain that binds ATP, and the nucleotide monophosphate (NMP)-binding domain that binds AMP. X-ray crystallographic studies showed that the LID and NMP domains undergo a major conformational rearrangement upon substrate binding (Figure 1a) (9-11). This movement, termed domain closure, forms the enzyme's active center and helps to exclude solvent molecules that might interfere with the chemical reaction. AK's domain-closure dynamics have been studied using NMR spectroscopy (6-8, 12) and fluorescence experiments (5, 6, 13), as well as multiple molecular dynamics simulations (14-19). In particular, our recent single-molecule FRET (smFRET) experiments demonstrated that AK's opening and closing rates are significantly faster than previously reported (20). In the presence of substrates, domain closure is completed in just a few tens of microseconds. These are likely the fastest large-scale conformational dynamics measured to date, and they are orders of magnitude faster than the overall turnover rate of the enzyme. It was proposed that these fast domain movements might assist the enzyme in orienting its substrates optimally for catalysis, a hypothesis supported by recent simulations (21).

Interestingly, AK also incurs a pronounced AMP-mediated substrate inhibition (SI) (22, 23). Despite many efforts, the mechanism behind SI has not been elucidated convincingly. While some studies have hinted toward the competitive binding of AMP at the ATP site (24), others claimed that AMP substrate inhibition in AK is uncompetitive in relation to ATP (22). Whether large-scale domain motions in AK relate to SI has also been debated. Bulk FRET studies have indicated that inhibition arises due to substantial closing of the LID domain upon AMP binding (23). However, it was unclear if this effect was induced by direct binding of AMP to the ATP site (competitive inhibition at the ATP site) or through allosteric modulation (i.e., AMP binding at its cognate site

affects LID domain movement). Other studies suggested that at high AMP concentrations, binding of AMP before the release of ADP from the LID domain might lead to the formation of an abortive complex that causes inhibition (22). The latter effect could arise if LID opening is slow and is the rate-limiting step in catalysis, as has been proposed (6, 12, 13).

In this work, we carried out experimental and computational studies on several inhibition-prone as well as non-inhibited mutants of AK (25) to determine the mechanism of AMP-mediated SI in AK. Based on the screening of an extensive AK mutant library, we show that mutations throughout the enzyme's structure modulate SI, suggesting that it has been under positive selection during evolution. We establish that inhibition cannot be explained by either competitive binding of AMP at the ATP site or spurious LID domain closure by AMP in the absence of ATP. Instead, we find that for inhibition-prone variants of AK, AMP facilitates domain closure at lower concentrations of ATP, which may interfere with proper substrate binding mechanics required for the reaction. Based on these results, we propose a kinetic model that combines conformational dynamics and chemical steps to explain the enzymatic activity of AK with substrate inhibition.

RESULTS

Structural and kinetic attributes of AK variants with substrate inhibition

In an earlier study (25), we characterized a series of mutants of AK and found a correlation between AMP-mediated SI and protein stability. An important question that arises is whether there is a specific region that is responsible for the gain or loss of SI, possibly by affecting how the substrates bind to the protein. To answer this, we created an extensive library of AK mutants and characterized their SI profiles. We particularly sought to identify mutations that alter SI without perturbing the enzymatic activity. Accordingly, using the crystal structure of AK with the bound inhibitor AP_5A (10), we first identified 71 residues that were at least 8Å away from the inhibitor and their sidechains were not involved in any interactions with the rest of the protein (Figure S1a, see details in Methods). We then generated a library of 923 mutants wherein 13 different amino acids were introduced at each of these 71 locations identified above (see Methods). Next, we developed a screening method (Figure S1b) to measure the extent of AMP-mediated SI directly from the cell lysate of 1248 individual colonies by measuring the ratio of the initial reaction velocity at two different concentrations of AMP (100 μM and 500 μM, Figure S1c).

We selected ~200 candidates from this dataset that showed lower, higher, and similar SI as the WT protein and sequenced them by Sanger sequencing to recover 86 unique mutations with clean chromatograms in the first pass. We further purified these proteins and measured their activity profiles. For a quantitative comparison between the mutants and literature values, the AMP-related Michaelis constant (K_M) and inhibition constant (K_I) were obtained by a fit to a model of uncompetitive inhibition (see Methods), and the values are given in Supplementary Table 1. We mapped the positions of the inhibition-prone mutants (K_I =< 500) and the non-inhibited mutants (K_I >= 1500) on the structure of AK (Figure 1b). Both effects can be observed for residues distributed all over the structure rather than in specific regions of the protein. We observed that at those locations where mutation led to a loss of inhibition, the WT residue had a statistically significant higher conservation (high frequency of occurrence in a multiple sequence alignment (26, 27)) than those that led to an increase of inhibition (Figure 1c). In other words, the gain of SI upon mutation tends to occur at positions of low conservation, while the loss of SI occurs at highly conserved locations. This signifies that SI in AK has been under positive selection during evolution. Since back-to-consensus mutations are generally stabilizing (28), this plot also signifies that higher protein stability generally leads to more SI in AK, as seen from our previous study (25).

The mutant screening experiment did not identify a specific structural attribute that is responsible for SI by AMP. Further, a crystallographic study of one of the mutants also did not demonstrate a structural change that may explain the effect of AMP. In particular, we determined the crystal structure of L107I AK, which shows strong inhibition, in complex with Ap_5A to a resolution of 2.05 Å. The structure was found to be very similar to other closed AK structures (10, 29, 30) (Figure S2), with a 0.3 Å root-mean-square deviation (RMSD) from the 1AKE structure (10). As no differences in the static structure of AK were found that could explain differences in enzymatic activity, these are more likely rooted in dynamic interactions. Therefore, we turned to studies of the dynamic properties of AK mutants in relation to SI.

From biochemistry to structural dynamics

To explain the origins of SI in AK and similar multi-substrate enzymes, previous studies have primarily considered three hypotheses. The first involved binding of the inhibiting substrate to an additional site (e.g. the ATP site) (31). The second, uncompetitive inhibition by AMP through blocking the accessibility of the ATP binding site (22, 23). Finally, it was suggested that kinetic

differences between alternating pathways towards the fully substrate-bound complex could lead to inhibition (32).

To probe the origins of SI further, we selected three variants of AK with similar thermal stabilities as the WT: L82V and L107I (25), which are more inhibited than the WT, and F86W, which is not inhibited by AMP (22). Michaelis-Menten curves for these variants as a function of AMP concentration are shown in Figure 1d. We first investigated if SI in AK arises due to AMP having a second binding site in addition to the one on the NMP domain. The additional binding site could be the ATP-binding site – as AMP is a close structural analog of ATP – or any other yet-unknown site. In that context, we found that for the WT (Figure S3a, Supplementary Table 2), the presence of excess ATP led to a gradual and dose-dependent loss in SI, which is a classic apparent sign of competitive inhibition at the ATP binding site. In other words, it seemed possible that the competitive binding of AMP at the ATP binding site at high concentrations causes inhibition, which is relieved by excess ATP in the solution. If this were true, then under conditions when the AMP concentration vastly surpasses the ATP concentration, binding of AMP to the ATP site would be preferred and result in a complete loss of activity. Contrary to this expectation, the enzyme retains significant residual activity even at high AMP concentrations (5, 22, 23), as seen particularly well for L107I (Figures 1d, S3b).

We therefore ask: does AMP inhibit AK by binding to the ATP binding site in the LID domain, or does it affect the catalytic properties differently? To gain insight into this question, we turned to smFRET spectroscopy to measure the domain movements directly. AK was labeled at residues 73 and 142, positioned in the CORE and LID domains, respectively (Figure 1a), and studied in solution (20). In the absence of substrates, AK molecules yielded a FRET efficiency histogram dominated by a peak at ~0.4 (Figure 2a, blue), corresponding to the open conformation. A shoulder towards higher FRET efficiency values indicated that the closed conformation is also sampled, though to a small extent (6, 20, 33). The addition of ATP (Figure 2a, green and purple) shifted the histogram towards higher FRET efficiency values, resulting from a considerable increase in the population of the closed conformation. In the presence of 1 mM AMP (orange), similar shifts were observed, but they required much lower concentrations of ATP.

Surprisingly, in the presence of high concentrations of AMP as a sole substrate, the FRET efficiency histogram of the WT protein remained unchanged (Figure 2b), indicating that AMP

alone cannot cause LID domain closure. To see if the effect of AMP is different in mutants with stronger or weaker SI, we also double-labeled the three variants introduced above (L107I, L82V and F86W). None of these single-point mutants significantly affected the FRET efficiency histogram of the apoenzyme (Figure S4a), and the addition of AMP alone did not induce a significant shift (Figure S4b). The only exception was L82V, the most inhibited mutant, which showed a slight shift towards higher FRET efficiencies. To accurately retrieve changes in the populations of the open and closed conformations of the enzyme under various conditions, we used the hidden-Markov model-based analysis method H^2MM (34). This algorithm employs photon arrival times as input for an optimization process that obtains both occupancies and rates of exchange of conformational states and is capable of retrieving microsecond dynamics. The model we used involved only two conformational states, open and closed (Figure 1a). A notable increase in the population of the closed state by AMP was seen only for L82V (Figure S5a). Interestingly, both closing (Figure S5b) and opening (Figure S5c) rates were accelerated in the binary AK-AMP complex. This effect was particularly substantial for L107I and L82V. In contrast, no changes were seen for the uninhibited F86W.

Clearly, AMP alone does not cause domain closure in AK. However, this does not rule out that AMP binds to the ATP site and blocks access for the native substrate, thereby inhibiting the protein. To check this point, we tested whether AMP can competitively replace ATP from its cognate binding site. To limit the potential effect of ADP, which binds to both the ATP and AMP site, we utilized the slowly hydrolyzable ATP analog ATP-γ-S. In the presence of 50 μM ATP-γ-S, partial closure was observed (Figure 2b). If AMP can displace ATP/ATP-γ-S from its native binding site, adding a vast excess of AMP should induce a shift towards the open conformation. Instead, we observed a minor shift towards the closed state in the FRET efficiency histograms, eliminating the possibility that AMP acts as a competitive substrate inhibitor.

To provide support to the point that AMP does not bind at the ATP site, in addition to the single-molecule studies, we rationally designed a mutant Q92Y that is predicted to weaken AMP binding at its cognate site, based on the structure of *E. coli* AK with bound Ap_5A (10). The mutation indeed led to a loss in activity for both the WT (Figure S6a) and L82V (Figure S6b). Using Differential Scanning Fluorimetry to obtain the change in thermal melting temperatures of AK upon ligand binding as a function of ligand concentration, we found that Q92Y on the background of WT

weakens AMP binding (Figure S6c). On the background of the highly inhibited mutant L82V (L82V-Q92Y mutant), it completely abolished AMP binding (Figure S6d), while ATP binding was retained for both WT and L82V backgrounds (Figure S6e-f). This experiment indicated that AMP cannot bind elsewhere to its cognate site.

AMP binding has an allosteric effect on the LID domain

Given the observed effect of AMP binding at its own site on LID domain dynamics, it is imperative to find whether AMP further modulates the effect of ATP on domain closure. Figure 2c-f shows how the population of the closed state of the enzyme changes with the concentration of ATP+ADP (with the latter's concentration chosen to maintain equilibrium in the enzymatic reaction), either without or with AMP. The very presence of ATP as a sole substrate (Figure 2c-f, circles) enabled a large conformational change from a predominantly open to a more closed conformation (maximum occupancy 56-78%). Fitting the curves in Figure 2c-f to simple binding isotherms provided the transition midpoint concentrations (which we call C_{50}), which were found to correlate with the strength of substrate inhibition (Supplementary Table 3). The impact of a fixed concentration of AMP on the ATP-dependent population of the closed state is shown in squares in Figure 2c-f. (In these experiments, ADP was added to maintain equilibrium in the enzymatic reaction; therefore, the combined concentration of ATP+ADP is depicted on the abscissa.) LID domain closure occurred at a 20-40 times lower substrate concentration in the presence of AMP (Supplementary Table 3), indicating remarkable cooperativity in substrate binding. This cooperativity was almost entirely absent for the non-inhibited mutant F86W (Figure 2f). Interestingly, previous work has shown that AMP binding reduces the K_M for ATP in the WT but not in the F86W mutant (22). The strongest cooperativity was observed for the most inhibited mutant, L82V (Figure 2e). Furthermore, in this mutant, the closed state was significantly more populated (78.4±0.7%) than for the WT (57.1±0.6%).

It is clear from the results of Figure 2 that AMP has an effect on the closure of the LID domain, even though it does not directly bind to that domain. AMP must therefore affect the LID domain allosterically. To shed further light on the effect of AMP on LID domain mechanics, we studied domain-closure dynamics at a fixed concentration of ATP (1 mM, together with specified concentrations of ADP to maintain equilibrium) and increased concentrations of AMP (Figure 3).

As reported earlier (20), both opening and closing rates are much faster than the enzymatic turnover (Supplementary Table 4). In the WT protein in the absence of AMP (Figure 3a), closing rates (27,307±752 s^{-1}) were slightly faster than opening rates (23,937±1,123 s^{-1}). Strikingly, the gradual addition of AMP did not affect the rate of domain opening. For the closing rate, small AMP concentrations – at which no inhibition is detected (up to ~1 mM) – also did not have a measurable impact. However, at inhibitory AMP concentrations (> 1 mM), domain closure was significantly accelerated (up to 50,289±2,795 s^{-1}), leading to a higher occupancy of the closed state of 63.5±0.4% (Figure S7). Interestingly, this overpopulation of the closed state coincided with the range of AMP concentrations where the most substantial drop in activity was observed (Figure 1b). A very similar picture was seen with the more inhibited variants (Figure 3b-c). No measurable impact of AMP binding was detected for the opening rates, whereas the closing rates increased above 100 μM. A C_{50} value of 2568±820 μM was found for the WT, with significantly lower values (~500 μM) for L107I and L82V. Moreover, L107I was shifted further towards the closed state (64.8±0.5%) than it is possible in the presence of ATP alone (55.8±0.8%). For L82V, the population of the closed state (75.5±0.8%) was the largest, which might match that mutant's overall low activity. No enhancement of the closing rate was detected for the non-inhibited mutant F86W (similar to Figure S5).

A model to explain substrate inhibition

Given that AMP inhibits AK's enzymatic activity and also affects domain-closure dynamics, we postulated that the two phenomena are correlated. Therefore, we devised a kinetic model for AK, based on the hypothesis that different closed states can be sampled, depending upon the order of ligand binding. Some of these states are incompatible with catalysis and must convert to the catalysis-prone state before the reaction occurs. As per our model (Figure 4a), the apoenzyme E can be present in both open (E^O, blue) and closed (E^C, red) states. (States are defined only for the ATP-binding LID domain.) The status of the LID domain does not affect the binding of AMP to the NMP domain; hence, both open and closed states can bind AMP. However, ATP can bind only to the open state.

If ATP binds first at the LID domain, the ET^O and ET^C, i.e. open and closed conformations of the ATP-bound protein, respectively, are formed. Both of these states can subsequently bind AMP and form a double substrate-bound state, ETM. If AMP binds first at the NMP domain to form EM^O

and EM^C, the consequent binding of ATP leads to the formation of ETM_{inh}. ETM and ETM_{inh} are distinguished by their binding order – ATP first, then AMP or vice versa- based on a hypothesis that initial AMP binding may result in a limited or different sampling of the relative orientation of the nucleotides (see below). Hence, ETM^C_{inh} is an unproductive closed state, while ETM^C is productive. The two ETM states can interconvert only through their open states, as suggested recently by MD simulations (21). At the same time, phosphoryl transfer can happen only through ETM^C. In essence, we have introduced a kinetic hindrance for the path that binds AMP first. When a typical activity assay of AK is carried out in the bulk in the presence of saturating ATP concentrations, at low AMP levels greater flux of the reaction goes through the pathway involving the productive ETM intermediate. However, as AMP levels increase, a larger fraction of the flux goes through the pathway involving the unproductive ETM_{inh} state, leading to a drop in activity.

To simulate kinetics based on this model, we used experimentally observed opening and closing rates of the LID domain for E ($E^O \rightleftharpoons E^C$), ET ($ET^O \rightleftharpoons ET^C$), EM ($EM^O \rightleftharpoons EM^C$), ETM ($ETM^O \rightleftharpoons ETM^C$) as input in the model (Supplementary Table 5). We assumed that each species has one specific opening and closing rate. The concentration of nucleotides determined the occupancy of each of these states (20). The single-molecule experiments could not distinguish between ET and ETM, as no change in the apparent protein dynamics was observed upon the addition of AMP at non-inhibiting concentrations (Figure 3). Therefore, the rates adopted for these two states were identical. The rates for the ETM_{inh} state ($ETM^O_{inh} \rightleftharpoons ETM^C_{inh}$) were derived from asymptotic values obtained from the binding isotherm fits of Figure 3 (Supplementary Note 1). We also assumed a single rate constant for the actual phosphotransfer step (1000 s^{-1}) and the conversion rate between ETM^O_{inh} and ETM^O (500 s^{-1}) for all mutants.

Under these model assumptions, a simulation of the enzyme activity at a saturating ATP concentration (1mM) and varying AMP concentrations (Figure 3b) was effectively able to reproduce the SI pattern of the WT as well as the mutants L107I and L82V. Further, no inhibition was observed for the F86W mutant, as expected. On the other hand, using a saturating AMP concentration (1mM) and varying ATP concentrations, the simulation did not show SI for any mutant (Figure 3c). The ability to obtain the correct level of inhibition by AMP for the different mutants provides strong support for the model.

We used the model to obtain some further insight into the role of domain closure dynamics in enzyme activity. To this end, we altered the rates of LID domain closing of each of the ETM states in turn, using one of two ways (Figure S8): either by preserving the open/closed ratio K_C or by preserving the opening rate, similar to the experimentally observed effect of AMP. In both scenarios, all other parameters were kept constant. As long as the equilibrium ratio K_C was preserved (Figure S8a), varying the closing rate towards the unproductive ETM^{O}_{inh} did not affect activity. With K_C preserved, also varying the rate towards the productive ETM^{C} had a minor effect (Figure S8b). A much more substantial impact of varying the closing rate towards ETM^{O}_{inh} was observed when the opening rate was fixed (Figure S8c). When the conformational equilibrium was altered, the unproductive states became more populated, which caused stronger inhibition. In contrast, for the productive closing (Figure S8d), enhancing the domain closure rate had a positive effect on turnover.

An important criterion determining SI strength is the conversion rate between ETM^{O}_{inh} and ETM^{O}. Figure S8e depicts how an increase in this rate can almost completely thwart SI while a reduction in the rate increases the effect. In our simulations (Figure 3c/d), we assumed a constant interconversion rate for all mutants, 500 s^{-1}. Still, the potent inhibition observed experimentally for L107I and L82V might also be influenced by a slower transition between ETM^{O}_{inh} and ETM^{O} for these mutants.

DISCUSSION

Despite its comparatively small size, AK's ubiquity and central role in cellular metabolism have attracted numerous studies. In particular, the complex interplay between conformational changes and enzymatic activity has been frequently investigated. An important aspect here is the AMP-mediated SI, which has been studied for several decades, but no mechanism has been conclusively established. In a previous work, several stabilizing and destabilizing point mutations were introduced into AK, and the mutants exhibited many extremes of SI (from very strong to no SI at all) (25). In the present work, we used several of those mutants (covering a range of SI behavior) to pinpoint a mechanism for inhibition. We show that neither uncompetitive nor competitive binding of AMP can explain SI in AK. Instead, we find that inhibition arises due to strong allosteric communication between the NMP and LID domains, which manifests in a highly cooperative closing of the LID domain for inhibition-prone mutants in the presence of both ligands (ATP and AMP) as compared to ATP alone. Based on this, we propose a model for the enzymatic activity that explains why greater sampling of the LID closed state in the presence of AMP and ATP might lead to SI. According to this model, the order of substrate binding matters. In particular, the initial binding of AMP followed by ATP leads to a closed state that does not allow the correct positioning of the ligands for effective phosphate transfer. Using the experimentally observed opening and closing rates for each state of the enzyme, this model can effectively reproduce the SI profiles of the different mutants studied. The enzymatic cycle of AK has traditionally been understood as a random bi-bi mechanism where the two substrates ATP and AMP can bind in any order. Our data shows that AK activity follows a particular class of random reactions: the substrates can bind in any order, but the outcome of the reaction is different along the two pathways.

Among the two inhibition-prone mutants, L82V displayed somewhat different properties than L107I. Being the most inhibition-prone, L82V showed an increase in closed-state occupancy with AMP alone, indicating that the allosteric communication between the LID and NMP sites is the highest in this mutant. Nevertheless, even for this mutant, opening rates are higher than closing rates in the presence of only AMP; hence, structural inaccessibility of the ATP binding site cannot be the reason for SI. In the presence of both AMP and ATP, the closed state occupancy for L82V is the highest among all mutants (78% vs. 63-65% for others), which is likely the reason for the

potent inhibition and overall low activity. In contrast, F86W displayed minimal impact of AMP on LID domain dynamics, and likewise, no inhibition.

Controlling the equilibrium between the open and closed state in AK provides a way to regulate enzymatic activity. Modulating this conformational equilibrium by other means, like mutations or osmolytes, was shown to affect enzymatic catalysis directly (20, 35). AMP also appears to be a major regulator of AK activity (35). In this context, we found that urea can lift AMP-mediated inhibition by repopulating the open state. We will focus on this effect in a future study.

The maximal catalytic rate of AK is obtained at or near the expected physiological concentration of AMP (35). Changes in AMP concentration will accordingly lead to changes in AK's activity, thus to an altered availability of nucleotides within the cell. In turn, this can substantially affect other processes in the cell. For example, we have recently shown that elevated AMP concentrations decrease the fitness of *E.coli* cells expressing inhibition-prone AK strains (25). The current work shows that SI has been under positive selection using an extensive library of AK mutants and subsequent informatics analyses. However, the precise beneficial role of regulating AK activity by AMP remains to be discovered. Additionally, our library data shows that SI can be modulated through mutations that span most regions of the proteins, suggesting that long-range allosteric communication is a general feature of AK.

It is important to mention that previous work on AK dynamics suggested that the LID opening rate is the rate-determining step in catalysis (12, 13). Our smFRET data in this study and the previous one (20) demonstrate that rates of domain movement (both opening and closing) are orders of magnitude faster than the enzymatic turnover, which implies that the enzyme opens and closes multiple times before the catalytic cycle is completed. Our model of the enzymatic activity coupled with conformational changes suggests that as long as these rates are substantially higher than the catalytic turnover rate (k_{cat}), the explicit interconversion rates between the open and closed states do not determine enzyme activity. Instead, the relative population of the two states is what determines activity and inhibition.

A matter of intense debate in enzyme catalysis is whether conformational fluctuations play a role in catalysis (2, 3, 36, 37). While several studies have claimed that enzyme fluctuations play a direct role in the chemical step, theoretical studies have refuted those (38). Our work suggests that the

ultrafast domain movements help to tune the equilibrium between states of the enzyme with different activities continuously. Such a mechanism is not unique to AK. For example, we recently discovered that the activity of the AAA+ disaggregation machine ClpB is tightly correlated to the distribution between active and inactive conformational states (39). However, the interconversion between these two states happens on a much faster timescale than any other protein activity (39). Schanda et al. found that the enzymatic activity of the TET2 aminopeptidase is controlled by the conformational equilibrium of a highly dynamic loop in the catalytic chamber (40). Also, the turnover in the HisFH enzyme complex is dictated by the population of the active state, with the conversion between ground and active state taking place on a faster time scale than enzymatic activity (41).

This study goes beyond previous attempts to connect conformational dynamics and chemical steps in enzymes by developing a kinetic model that explicitly takes conformational changes into account. The model builds on the recent *in silico* observation that fast opening and closing cycles might help to find the correct mutual substrate orientation efficiently and to guarantee the high catalytic activity of the enzyme (21). It is further based on the hypothesis that *the order of binding of the two substrates to the enzyme* dictates how effectively repeated opening and closing cycles help to reorientate the substrates for the reaction. Strikingly, this model is able to correctly reproduce trends of substrate inhibition among the WT enzyme and several mutants. In conclusion, our study of a common and widely studied enzyme uncovers the mechanistic relationship between very fast conformational variation and catalysis.

ACKNOWLEDGMENTS

The work of G.H. was supported by a grant from the European Research Council (ERC) under the European Union's Horizon 2020 Research and Innovation Program (grant agreement No 742637, SMALLOSTERY) and a grant from the Israel Science Foundation (no. 1250/19). The work of D.S. was supported by Deutsche Forschungsgemeinschaft (DFG, German Research Foundation, Projektnummer 490757872). The work of E.G. was supported by the National Institute of Health (NIH) grant 5R35GM139571.

Figure legends:

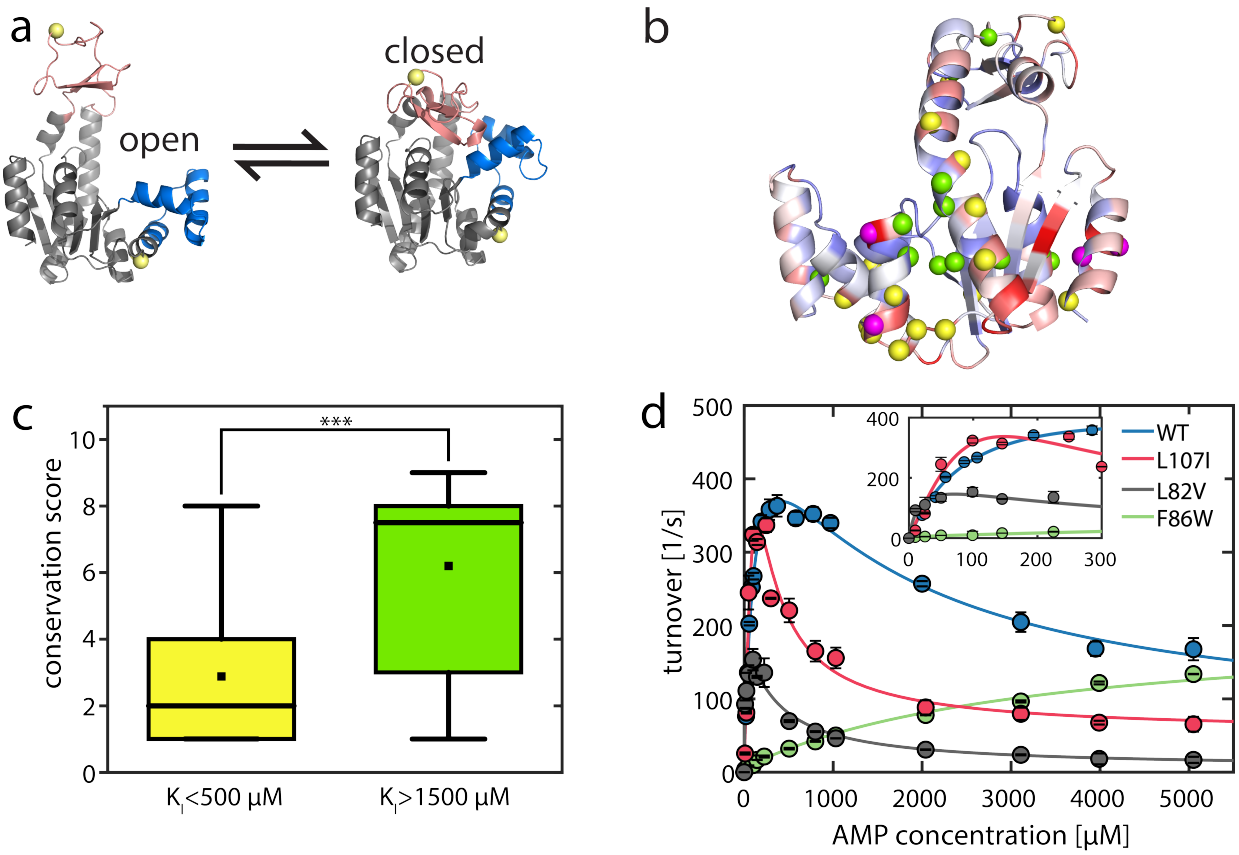

Figure 1. Structural and kinetic attributes of AK variants. (a) Structure of AK with its three domains. The CORE domain (grey) connects the LID domain (pink) and the NMP domain (blue). The yellow spheres indicate the positions for the attachment of fluorescent dyes. The protein can undergo a conformational change from the open state (left, PDB 4AKE) towards the closed conformation (right, PDB 1AKE). (b) Conservation score mapped onto the open state with high to low conservation represented as blue to red. The positions with mutants having a K_I <=500 µM for AMP are shown as yellow spheres, while those with K_I >=1500 µM are shown in green. The four magenta spheres are positions where both inhibited and uninhibited mutations are observed (see Supplementary Table 1). The conservation scores were obtained from the ConSurf web server (26, 27). (c) Distribution of the conservation scores in both strong and weak inhibition bins. The mutations that result in strong inhibition (K_I <=500) usually occur at less conserved positions (2.9±0.6), while inhibition-relieving mutations (K_I >=1500) occur mostly at highly conserved

positions (6.2±0.9). (d) Activity curves of WT AK and selected mutants show increased SI (L107I, L82V) or loss of inhibition (F86W).

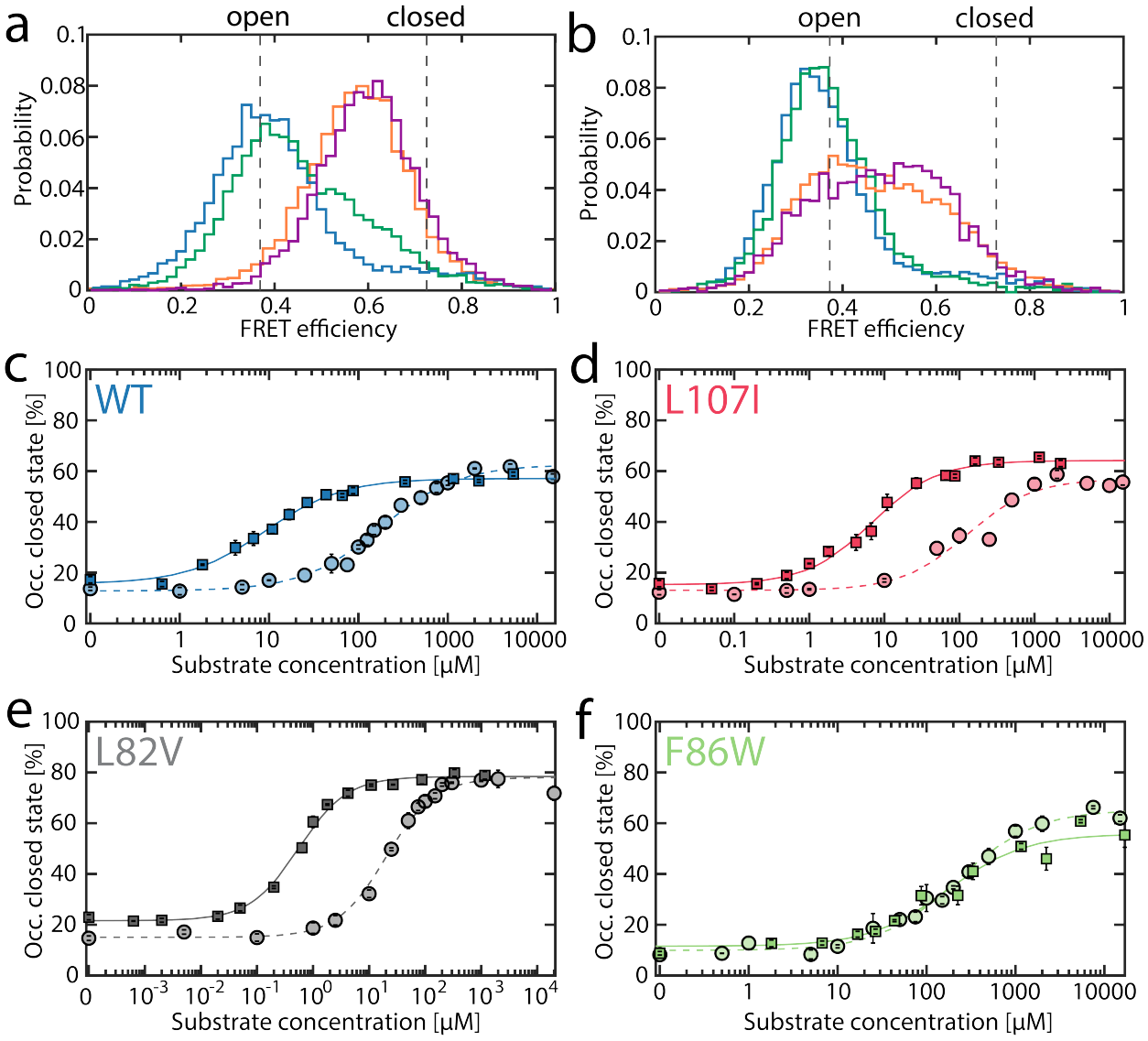

Figure 2. ATP-dependent closure of the LID domain. a-b) FRET efficiency histograms of the WT protein. (a) The apoprotein (blue trace) mainly adopts an open conformation, occasionally exploring the closed state. The binding of ATP increases the population of the closed state, as demonstrated by histograms at 100 μM (green) and 1 mM (purple) ATP. When 1 mM AMP is added, a significant population of the closed state is attained even at a low ATP concentration of 50 μM (orange). In this experiment, ADP was also added at concentrations that maintained the equilibrium of the enzymatic reaction (20). The dashed lines indicate the most likely positions of the open and closed state based on data analysis (see below). (b) AMP alone, even at 30 mM (green), leads to very minimal changes in FRET efficiency compared to the apoprotein (blue). ATP-γ-S, a slowly hydrolyzable analog of ATP, binds to the ATP binding site and triggers partial

closure at 50 µM (orange). In the presence of both ligands (purple), ATP-γ-S is still bound to the ATP-binding site and not outcompeted by AMP, which would trigger LID opening. Instead, the binding of AMP to its own site even promotes closure to a minor extent. c-f) The occupancy of the closed state was determined by H^2MM in the presence of either solely ATP (circles) or also 1 mM AMP (squares). In all variants, the LID domain closes at high ATP levels. For (c) WT, (d) L107I and (e) L82V, the presence of 1 mM AMP promotes closure at much lower ATP concentrations. In the non-inhibited mutant (f) F86W, AMP has no significant effect. Dashed (ATP only) and straight (all substrates) lines indicate fits to a binding model as described in Supplementary Note 1. Error bars are given as the standard error of the mean of repeated measurements. In (c-f), as above, ADP was added to maintain equilibrium; the substrate concentration on the abscissa is the total concentration of ligands for the ATP binding site (i.e. ATP+ADP).

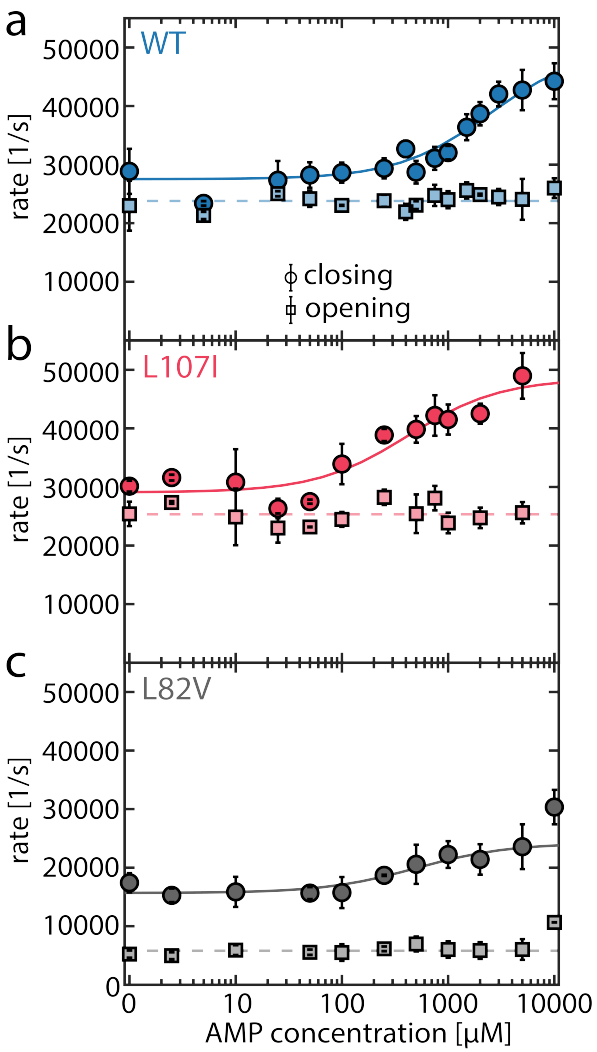

Figure 3: AMP accelerates LID domain closing. Opening (circles, solid lines) and closing (squares, dashed lines) rates for a) the WT (blue), b) L107I (red) and c) L82V (grey) in the presence of increasing concentrations of AMP and a fixed concentration of ATP (1 mM). Opening rates are not affected by the presence of AMP. The closing rates were fitted to a model described in Supplementary Note 1. Error bars are given as the standard error of the mean of repeated measurements.

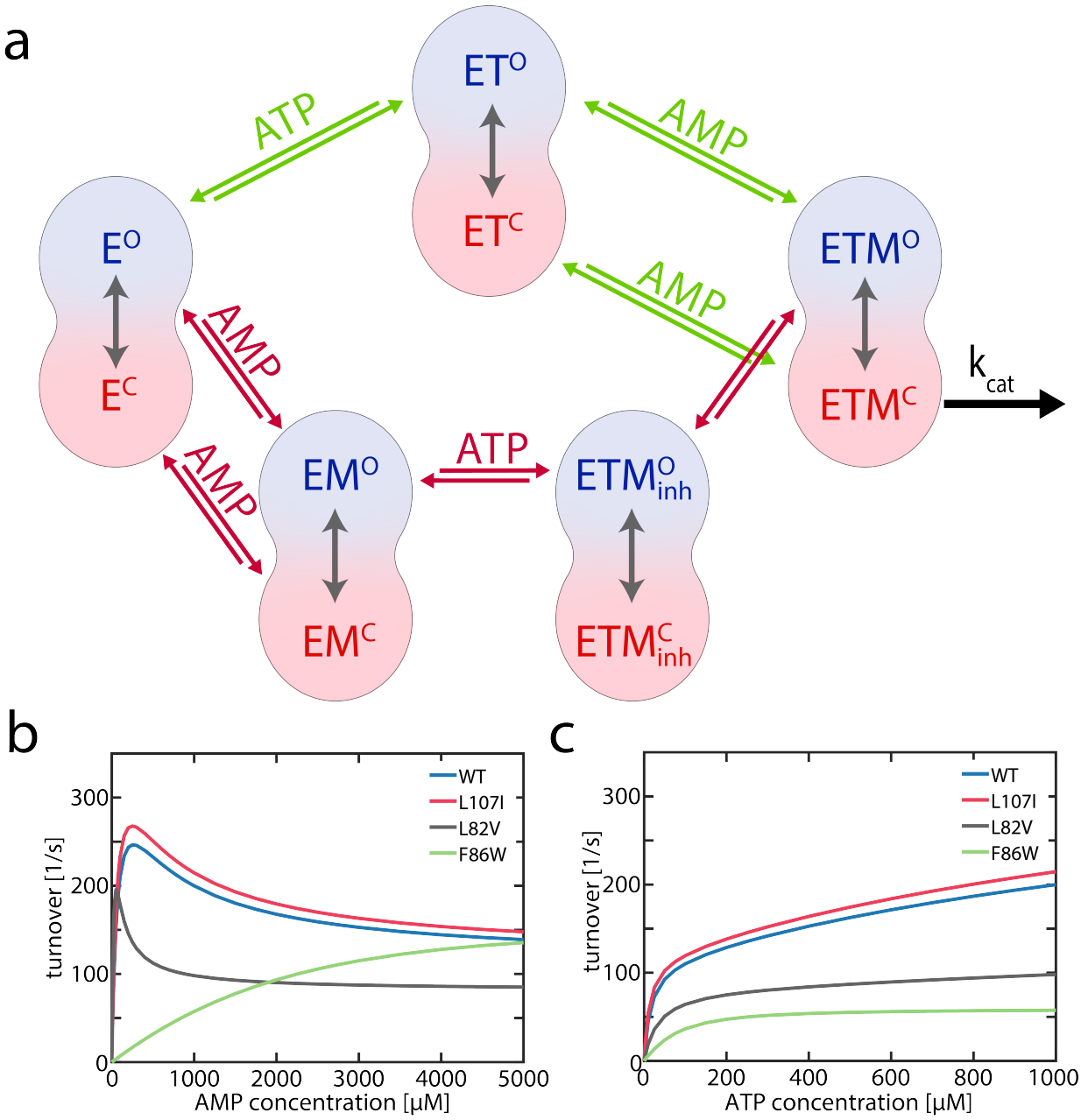

Figure 4: A model to explain substrate inhibition. (a) Scheme of the model, which is based on two competing pathways: When ATP binds first (green pathway) to the apoenzyme (E), this results in the ATP-bound state ET. Subsequent binding of AMP leads to a productive closed state (ETM) that undergoes the chemical step of the enzyme in the closed conformation (ETM^C). However, if AMP binds first (red pathway, via EM), subsequent binding of ATP causes the formation of ETM_{inh}, which deviates from the productive state ETM in the orientation of the substrates. It is assumed that the closed state ETM^C_{inh} does not enable phosphotransfer due to an inappropriate

substrate orientation. The corresponding open conformation ETM^{O}_{inh} must convert to ETM^{O} to enable catalysis. Binding or reorientation of ATP, which lead to a productive catalytic conformation, cannot occur in the closed conformation (21). (b-c) Simulated activity curves of WT and mutants as a function of (b) AMP and c) ATP concentrations based on the model (a) and experimentally observed parameters of opening and closing rates. The rate of conversion from $ETM1^{O}$ to $ETM2^{O}$ was fixed at 500 s^{-1}. The model shows AMP-mediated SI for WT, L107I and L82V, but not for F86W. No SI was observed as a function of ATP concentration, in accordance with experimental data.

References:

1. D. Thirumalai, C. Hyeon, P. I. Zhuravlev, G. H. Lorimer, Symmetry, Rigidity, and Allosteric Signaling: From Monomeric Proteins to Molecular Machines. *Chem. Rev.* **119**, 6788-6821 (2019).
2. A. Warshel, R. P. Bora, Perspective: Defining and quantifying the role of dynamics in enzyme catalysis. *The Journal of chemical physics* **144**, 180901 (2016).
3. K. Henzler-Wildman, D. Kern, Dynamic personalities of proteins. *Nature* **450**, 964-972 (2007).
4. R. Callender, R. B. Dyer, The dynamical nature of enzymatic catalysis. *Accounts of chemical research* **48**, 407-413 (2015).
5. M. A. Sinev, E. V. Sineva, V. Ittah, E. Haas, Domain Closure in Adenylate Kinase. *Biochemistry* **35**, 6425-6437 (1996).
6. K. A. Henzler-Wildman *et al.*, Intrinsic motions along an enzymatic reaction trajectory. *Nature* **450**, 838-844 (2007).
7. T. P. Schrank, D. W. Bolen, V. J. Hilser, Rational modulation of conformational fluctuations in adenylate kinase reveals a local unfolding mechanism for allostery and functional adaptation in proteins. *Proceedings of the National Academy of Sciences* **106**, 16984-16989 (2009).
8. M. Kovermann *et al.*, Structural basis for catalytically restrictive dynamics of a high-energy enzyme state. *Nature communications* **6**, 7644-7644 (2015).
9. G. E. Schulz, C. W. Müller, K. Diederichs, Induced-fit movements in adenylate kinases. *Journal of Molecular Biology* **213**, 627-630 (1990).
10. C. W. Müller, G. E. Schulz, Structure of the complex between adenylate kinase from Escherichia coli and the inhibitor Ap5A refined at 1.9 Å resolution: A model for a catalytic transition state. *Journal of molecular biology* **224**, 159-177 (1992).
11. C. Vonrhein, G. J. Schlauderer, G. E. Schulz, Movie of the structural changes during a catalytic cycle of nucleoside monophosphate kinases. *Structure* **3**, 483-490 (1995).
12. M. Wolf-Watz *et al.*, Linkage between dynamics and catalysis in a thermophilic-mesophilic enzyme pair. *Nature structural & molecular biology* **11**, 945-949 (2004).
13. J. A. Hanson *et al.*, Illuminating the mechanistic roles of enzyme conformational dynamics. *Proceedings of the National Academy of Sciences* **104**, 18055-18060 (2007).
14. J. Lee, K. Joo, B. R. Brooks, J. Lee, The atomistic mechanism of conformational transition of adenylate kinase investigated by Lorentzian structure-based potential. *Journal of chemical theory and computation* **11**, 3211-3224 (2015).
15. W. Li, J. Wang, J. Zhang, S. Takada, W. Wang, Overcoming the Bottleneck of the Enzymatic Cycle by Steric Frustration. *Physical Review Letters* **122**, 238102 (2019).
16. Y. Zheng, Q. Cui, Multiple Pathways and Time Scales for Conformational Transitions in apo-Adenylate Kinase. *Journal of Chemical Theory and Computation* **14**, 1716-1726 (2018).
17. P. C. Whitford, O. Miyashita, Y. Levy, J. N. Onuchic, Conformational Transitions of Adenylate Kinase: Switching by Cracking. *Journal of Molecular Biology* **366**, 1661-1671 (2007).
18. E. Formoso, V. Limongelli, M. Parrinello, Energetics and Structural Characterization of the large-scale Functional Motion of Adenylate Kinase. *Scientific Reports* **5**, 8425 (2015).
19. P. Maragakis, M. Karplus, Large Amplitude Conformational Change in Proteins Explored with a Plastic Network Model: Adenylate Kinase. *Journal of Molecular Biology* **352**, 807-822 (2005).
20. H. Y. Aviram *et al.*, Direct observation of ultrafast large-scale dynamics of an enzyme under turnover conditions. *PNAS* **115**, 3243-3248 (2018).
21. J. Lu, D. Scheerer, W. Wang, G. Haran, W. Li, Role of repeated conformational transitions in substrate binding of adenylate kinase. *The Journal of Physical Chemistry B* **126**, 8188-9201 (2022).

22. P. Liang, G. N. Phillips Jr., M. Glaser, Assignment of the nucleotide binding sites and the mechanism of substrate inhibition of Escherichia coli adenylate kinase. *Proteins: Structure, Function, and Bioinformatics* **9**, 28-36 (1991).
23. M. A. Sinev, E. V. Sineva, V. Ittah, E. Haas, Towards a mechanism of AMP-substrate inhibition in adenylate kinase from Escherichia coli. *FEBS Letters* **397**, 273-276 (1996).
24. J. Reinstein *et al.*, Fluorescence and NMR investigations on the ligand binding properties of adenylate kinases. *Biochemistry* **29**, 7440-7450 (1990).
25. B. V. Adkar, S. Bhattacharyya, A. I. Gilson, W. Zhang, E. I. Shakhnovich, Substrate inhibition imposes fitness penalty at high protein stability. *PNAS* **116**, 11265-11274 (2019).
26. H. Ashkenazy, E. Erez, E. Martz, T. Pupko, N. Ben-Tal, ConSurf 2010: calculating evolutionary conservation in sequence and structure of proteins and nucleic acids. *Nucleic acids research* **38**, W529-W533 (2010).
27. H. Ashkenazy *et al.*, ConSurf 2016: an improved methodology to estimate and visualize evolutionary conservation in macromolecules. *Nucleic acids research* **44**, W344-W350 (2016).
28. B. T. Porebski, A. M. Buckle, Consensus protein design. *Protein Eng Des Sel* **29**, 245-251 (2016).
29. M. B. Berry *et al.*, The closed conformation of a highly flexible protein: The structure of E. coli adenylate kinase with bound AMP and AMPPNP. *Proteins: Structure, Function, and Bioinformatics* **19**, 183-198 (1994).
30. M. B. Berry, E. Bae, T. R. Bilderback, M. Glaser, G. N. Phillips Jr., Crystal structure of ADP/AMP complex of Escherichia coli adenylate kinase. *Proteins: Structure, Function, and Bioinformatics* **62**, 555-556 (2006).
31. J. Reinstein *et al.*, Fluorescence and NMR investigations on the ligand binding properties of adenylate kinases. *Biochemistry* **29**, 7440-7450 (1990).
32. W. Ferdinand, The interpretation of non-hyperbolic rate curves for two-substrate enzymes. A possible mechanism for phosphofructokinase. *Biochemical Journal* **98**, 278-283 (1966).
33. M. Kovermann, C. Grundström, A. E. Sauer-Eriksson, U. H. Sauer, M. Wolf-Watz, Structural basis for ligand binding to an enzyme by a conformational selection pathway. *Proceedings of the National Academy of Sciences* **114**, 6298-6303 (2017).
34. M. Pirchi *et al.*, Photon-by-photon hidden Markov model analysis for microsecond single-molecule FRET kinetics. *J. Phys. Chem. B* **120**, 13065-13075 (2016).
35. R. J. Huss (1985) Regulation of adenylate kinase. (University of Illinois at Urbana-Champaign, Ann Arbor), p 129.
36. G. Bhabha *et al.*, A Dynamic Knockout Reveals That Conformational Fluctuations Influence the Chemical Step of Enzyme Catalysis. *Science* **332**, 234-238 (2011).
37. E. Z. Eisenmesser *et al.*, Intrinsic dynamics of an enzyme underlies catalysis. *Nature* **438**, 117-121 (2005).
38. A. Warshel, R. P. Bora, Perspective: Defining and quantifying the role of dynamics in enzyme catalysis. *J Chem Phys* **144**, 180901 (2016).
39. H. Mazal *et al.*, Tunable microsecond dynamics of an allosteric switch regulate the activity of a AAA+ disaggregation machine. *Nat. Commun.* **10**, 1438 (2019).
40. D. F. Gauto *et al.*, Functional control of a 0.5 MDa TET aminopeptidase by a flexible loop revealed by MAS NMR. *Nature communications* **13**, 1-13 (2022).
41. J. P. Wurm *et al.*, Molecular basis for the allosteric activation mechanism of the heterodimeric imidazole glycerol phosphate synthase complex. *Nature Communications* **12**, 2748 (2021).